



Augmenting Neuromuscular Disease Detection Using Optimally Parameterized Weighted Visibility Graph

Rohit Bose , Student Member, IEEE, Kaniska Samanta , Sudip Modak , and Soumya Chatterjee 

Abstract—In this contribution, we propose a novel neuromuscular disease detection framework employing weighted visibility graph (WVG) aided analysis of electromyography signals. WVG converts a time series into an undirected graph, while preserving the signal properties. However, conventional WVG is sensitive to noise and has high computational complexity which is problematic for lengthy and noisy time series analysis. To address this issue in this article, we investigate the performance of WVG by varying two important parameters, namely penetrable distance and scale factor, both of which have shown promising results by eliminating the problem of signal adulteration and decreasing the computational complexity, respectively. We also aim to unfold the combined effect of these two aforesaid parameters on the WVG performance to discriminate between myopathy, amyotrophic lateral sclerosis (ALS) and healthy EMG signals. Using graph theory based features we demonstrated that the discriminating capability between the three classes increased significantly with the increase in both penetrable distance and scale factor values. Three binary (healthy vs. myopathy, myopathy vs. ALS and healthy vs. ALS) and one multiclass problems (healthy vs. myopathy vs. ALS) have been addressed in this study and for each problem, we obtained optimum parameter values determined on the basis of F-value computed using one way analysis of variance (ANOVA) test. Using optimal parameter values, we obtained mean accuracy of 98.57%, 98.09% and 99.45%, respectively for three binary and 99.05% for the multi-class classification problem. Additionally, the computational time was reduced by 96% with optimally selected WVG parameters compared to traditional WVG.

Index Terms—Electromyography signals, weighted visibility graph, myopathy, ALS, penetrable distance, scale factor.

Manuscript received January 2, 2020; revised April 15, 2020 and June 3, 2020; accepted June 4, 2020. Date of publication June 11, 2020; date of current version March 5, 2021. (Corresponding author: Rohit Bose.)

Rohit Bose is with the Rehab Neural Engineering Labs, Department of Bio-Engineering, University of Pittsburgh, Pittsburgh, PA 15260 USA (e-mail: rohitbose94@gmail.com).

Kaniska Samanta, Sudip Modak, and Soumya Chatterjee are with the Department of Electrical Engineering, Techno India University, Kolkata 700091, India (e-mail: kaniska.samanta@gmail.com; sudipmodak9@gmail.com; chapeswar@gmail.com).

This article has supplementary downloadable material available at <https://ieeexplore.ieee.org>, provided by the authors.

Digital Object Identifier 10.1109/JBHI.2020.3001877

I. INTRODUCTION

ELECTROMYOGRAPHY (EMG) signal is a type of bio potential generated due to skeletal muscle activity and associated nerve cells. In hospitals and clinics, EMG has been extensively used for clinical diagnosis of several neuromuscular diseases like myopathy, amyotrophic lateral sclerosis (ALS) etc. Myopathy is a neuromuscular disease caused due to abnormal functioning of muscle fiber tissues attached to skeletal muscles [1]. ALS causes rapid degradation of nerve cells, eventually leading to death of motor neurons [2]. Hence, accurate detection of neuromuscular disorders is crucial for early diagnosis of these diseases. Visual inspection of EMG signals by doctors, to detect salient characteristics of such neuromuscular diseases from EMG signals lacks is time-consuming and sometimes inaccurate. To address this issue, different advanced signal processing and machine learning algorithms have been proposed by the researchers for fast and accurate computer aided detection of neuromuscular disorders.

Past literatures have reported neuromuscular disease detection using suitable features extracted from EMG signals. Time domain analysis of EMG signals using cross-correlation [1], autoregressive cepstral analysis [3] has been reported in existing literatures for detection of neuromuscular disorders. Frequency domain analysis of EMG signals using fast Fourier transform (FFT) [4], mel frequency of cepstral coefficients [5] has also been reported in existing literatures. Joint time frequency domain analysis of EMG signals employing short time Fourier transform (STFT) [6], continuous (CWT) [7] and discrete wavelet transform (DWT) [2], Stockwell transform (ST) [8] tunable Q-factor wavelet transform (TQWT) [9], empirical mode decomposition [10] etc. has also been reported in existing literatures. EMG signal classification using non-linear features like multiscale entropy [11], approximate entropy, correlation dimension, Hurst exponent, fractal dimension and largest Lyapunov exponent was reported in [12]. Recently, time series analysis using visibility graph has proven to be an emerging area of research for understanding non-linear system dynamics [13], [14]. Considering the above fact, in this study we investigate the feasibility of using visibility graph for analysis EMG signals.

Visibility graph (VG) proposed by Lacasa et al. in [15] is an effective algorithm for mapping a univariate time series into an undirected graphical representation. Using VG any time series can be converted to a complex network. However, one limitation

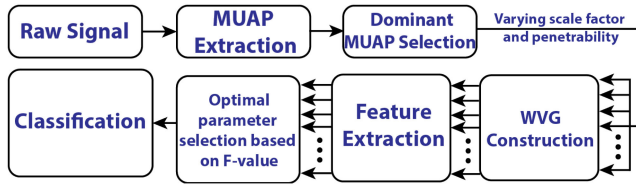


Fig. 1. Outline of the proposed method for EMG signal classification.

of the conventional VG algorithm is that it only provides information regarding node wise connectivity, but fails to provide any information regarding the weights of the individual edges in a connected graph. Considering this issue, VG with edge weights also known as weighted visibility graph (WVG) has been proposed by Supriya et al. in [16] where edge weights were introduced based on the absolute gradient values between two connected nodes. Application of WVG for analysis of physiological signal analysis like EEG [8], [17], [18], EMG [19] etc. has been reported in existing literatures. Although WVG is an upgraded version of conventional VG, yet traditional WVG has two major drawbacks: Firstly, it is sensitive to noise and secondly, dealing with such large data points incorporates high computational complexity. Recently, concepts of penetrable distance [20], [21] and scale factor [22] were introduced with an aim to solve these drawbacks. Penetrable distance enhances the network's robustness against noise [20]. Varying the scale factor helps to reduce the time series complexity which improves the performance of the network [23]. However, the effect of the varying these two parameters on the performance of WVG in a collective manner is also not known.

Considering the aforesaid fact, in this study, our primary goal is to observe the effect of varying penetrable distance and scale factor simultaneously on the performance of WVG to discriminate between myopathy, ALS, and healthy EMG signals. To the best of the authors' knowledge this is the first study where that the interaction between penetrable distance and scale factor of WVG has been investigated thoroughly for diagnosis of neuromuscular disorders. In the present contribution, we performed a grid search of penetrable distance and scale factor values to construct the WVG from the EMG time series. For each pair of the parameter values, we extracted four graph theory based features clustering coefficient (CC), global efficiency (GE), local efficiency (LE) and Transitivity (TR), and evaluated the F-values from the ANOVA test between all possible pairs of the three binary classes and one multi-class problem. We selected the optimum penetrable distance and scale factor that yielded the highest F-values between different classes and the corresponding feature values were used for classification. We observed that the proposed method returned very high classification accuracy in discriminating different class of EMG signals for all test cases. A flowchart of our proposed method is shown in Fig. 1.

II. DATASET DESCRIPTION

A publicly available EMG signal database has been used for this study [24]. The dataset consists of normal control group with 10 healthy subjects (4 females and 6 males, age 21 to

37 years) with no history of any kind of neurological disorder, 7 Myopathy patients (5 males and 2 females, age 19 to 63 years) and 8 ALS patients (4 males and 4 females, age 37 to 67 years). All the EMG signals were acquired from brachial biceps muscle and were digitized at a sampling frequency of 23.438 kHz. The recordings were made at low (just above threshold) voluntary and constant level of contraction by using a standard concentric needle electrode with three different level of insertion (deep, medium, low) at five different places of the muscles. The cutoff frequencies of high and low pass filters of the EMG amplifier set to 2 Hz and 10 kHz respectively. In this study, we have used the entire dataset consisting of 484 signals (284 healthy, 104 myopathy and 96 ALS) for analysis.

A. Pre-processing of EMG data

After acquisition of EMG data, we divided the signal into 25 segments with each segment containing 4096 data points. From each segment we extracted the motor unit action potentials (MUAP) using the EMGLAB software [25]. The software determines template MUAPs from the initial 2 sec of the EMG data. The criterion to select a template is that, it has to occur at least three times with high similarity. Manual inspection was performed for each template to ensure that the templates determined by the toolbox were accurate. Based on that template, similar MUAPs were grouped together. Further details of the MUAP extraction process using EMGLAB software can be obtained in [25]. Now, after extraction of constituent MUAPs from EMG signals, we selected the most dominant MUAP for each class. For this purpose, we calculated the signal energy of each extracted MUAPs for a particular EMG signal using Parseval's theorem. The MUAP with the highest signal energy is selected as the most dominant MUAP [2]. This process is repeated for all the EMG signals to obtain the dominant MUAPs for each class of EMG signals containing 625 data points. For, each class we obtained 2400 dominant MUAPs on which WVG was constructed for the purpose of analysis.

III. METHODOLOGY

A. Weighted Visibility Graph

The weighted visibility graph (WVG) proposed by Supriya et al. in [16] is a modification of conventional VG originally formulated by Lacasa et al. in [16]. Let a time-series of N number of data points, $\{x(i), i = 1, 2, 3, \dots, N\}$ is mapped into a graphical network where the number of nodes present in a graph represent the corresponding data points. For visibility to exist between two data points a and b , each point c lying in between them must satisfy the following condition

$$n_c < n_b + (n_a - n_b) \frac{m_b - m_c}{m_b - m_a} \quad (1)$$

Where (m_a, n_a) and (m_b, n_b) are the co-ordinates of the data points a and b , respectively and that of the intermediate data point c is (m_c, n_c) as shown in Fig. 2. If an edge is present, then the gradient of the visibility line connecting two data points forms the weight of that edge. The VG with edge weights is known as weighted visibility graph (WVG). Let us consider a random time

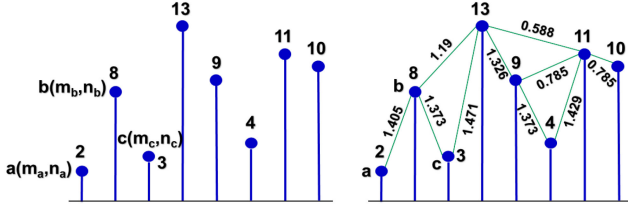


Fig. 2. WVG of a time series with edge weights.

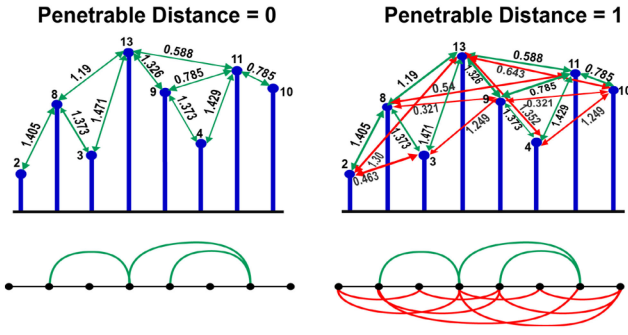


Fig. 3. Effect of penetrable distance of WVG of a time series.

series given by $X = \{2, 8, 3, 13, 9, 4, 11, 10\}$. The edge weight w_{ab} between two nodes (a, b) (see Fig. 2) are computed using (2), where the weights are expressed in radians.

$$w_{ab} = \left| \tan^{-1} \left(\frac{n_b - n_a}{m_b - m_a} \right) \right| \quad (2)$$

1) **Penetrable Distance**: The concept of penetrable distance was proposed to enhance the robustness of the VG to signal noises. We consider the same time series of Fig. 2 with the penetrable distance denoted by ρ . The penetrable distance allows two nodes of the graph to be connected even if one or more data points are present in between them, shown in Fig. 3.

The value of ρ decides the number of data points that are allowed to be ignored even if they are blocking the connecting (visibility) line between two nodes. For example, if we consider $\rho = 0$, we get the traditional WVG. When $\rho = 1$, an edge will be present between two nodes if there at most one data point obstructing the visibility line connecting the two nodes (marked in red in Fig. 3). Thus, penetrable distance enables WVG to neglect one or more intermediate data points which may be present due to noise.

2) **Scale Factor (SF)**: Analysis of time series in multiple scales has been widely used by researchers to reduce the signal complexity [23]. Furthermore, it can also help to reduce noise present in a signal. Mathematical expression of scale factor is given by [22]

$$S^k(n) = \frac{1}{k} \sum_{m=(n-1)k+1}^{nk} x(m) \quad \text{when } 1 \leq n \leq N/k \quad (3)$$

Where k represents as scale factor and m, n are randomly selected data points. Fig. 4 illustrates a portion of the same time series (used in Fig. 2 and Fig. 3) computed for two different values of SF ($SF = 1$ and $SF = 2$), respectively. As it can be

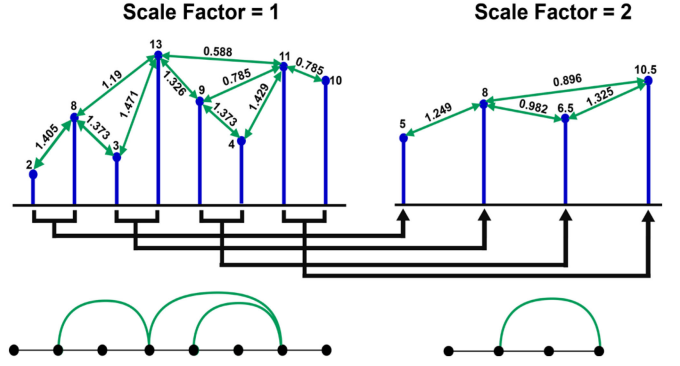


Fig. 4. Effect of scale factor on WVG of a time series.

seen from Fig. 4, the mean of two or more consecutive data points are taken depending on the SF to minimize the large number of data points. Therefore, introducing SF has smoothing effect on a signal. For WVG, with $SF = 1$, we get traditional WVG (see Fig. 3). But for $SF = 2$, WVG pattern is changed as new WVG (or signal). Also, the connectivity between different nodes is reduced which can reduce the complexity of the time series.

B. Feature Extraction

1) **Clustering Coefficient**: The clustering coefficient (CC) signifies how many triangles are being formed i.e. how well the neighboring nodes are connected with each other with respect to a particular node. It symbolizes small well interconnected local groups in a network [26]. The local CC for particular i th node C_i and the average clustering coefficient C_a was calculated using (4) and (5), respectively.

$$C_i = \frac{t_i}{d_i(d_i - 1)} \quad (4)$$

$$C_a = \frac{1}{N} \sum_{i=1}^N C_i \quad (5)$$

Where t_i stand for weighted geometric mean of the triangles for i th node and d_i stands for the weighted degree of the i th node and N denotes the node number of the constructed using WVG.

2) **Efficiency**: Efficiency of a graph is defined as the measure of the capability of the network to exchange information [27]. The concept of efficiency is applicable in both global and local perspective. Global Efficiency (GE) quantifies the exchange of information across the entire network. On the other hand, local efficiency (LE) is defined as the node wise quantification of the exchange of information with its neighboring nodes. We calculated GE and LE using (6) and (7), respectively.

$$GE = \frac{1}{Q(Q-1)} \sum_{i,j \in Q} \frac{1}{L_{ij}} \quad (6)$$

$$LE = \frac{1}{Q(Q-1)} \sum_{i,j \in Q} \frac{1}{L_{ij}} \quad (7)$$

Here, Q represents the size of graph and L_{ij} denotes the shortest path length.

TABLE I
TYPES OF CLASSIFICATION PROBLEMS

CP	Description
I	healthy vs. ALS
II	healthy vs. myopathy
III	ALS vs. myopathy
IV	healthy vs. ALS vs. myopathy

3) *Transitivity*: Transitivity measures the probability that all the neighboring nodes of a network are interconnected. (TR) can be computed from the following expression [19]

$$T = \frac{3 \times T_r}{T_p} \quad (8)$$

Where T_r is the number of triangles present in the network and T_p is the number of connected triplets of vertices.

C. Naive Bayes Classifier

Naive Bayes (NB) classifier is a very popular and widely used machine learning algorithm. This algorithm sets apart two classes by assuming the features are independent given class by employing Bayes' theorem and maximum posteriori hypothesis. The advantage of using NB classifier is that the classifier is robust against outliers and can ignore irrelevant features. Besides, due to its probabilistic framework, it updates quickly in addition of new data points. Both factors help to obtain better performance and also facilitate translation to clinical studies as noisy trials and updating model with new information is a critical aspect. Details about NB classifier have been reported in [28]. Application of NB to classify bio-signals has been reported in existing literatures [29]. Hence, NB classifier is used here to classify EMG signals.

IV. RESULTS

In this study, we performed four classification problems (CP) which are described in Table I. CP-I and II are binary classification tasks that can distinguish healthy from ALS and myopathy patients, respectively. CP-III is another binary classification problem that can distinguish between ALS and myopathy EMG signals. Finally CP-IV is a multiclass problem that can discriminate healthy, myopathy and ALS signals simultaneously.

To optimize the parameters of WVG, in this study, we used a grid search of ρ and SF values. The algorithm sweeps across a range of parameter values with a specific step size. In this study, the SF was varied from 1 to 25 with a step size of 1, and the ρ was varied from 0 to 7 with a step size of 1. Hence for each CP, 200 (25×8) experimental conditions were achieved which results in 200 sets of features computed from WVGs for different combinations of ρ and SF . For each combination, we performed one-way analysis of variance (ANOVA) test. The F-value obtained from ANOVA test was used as a measure to quantify the difference between the three classes of EMG signals and the optimum value of ρ and SF were selected for each feature that returned highest F-value between three classes. The F-value is chosen as a criterion in this study because it signifies how much the population means of the groups is different. It should

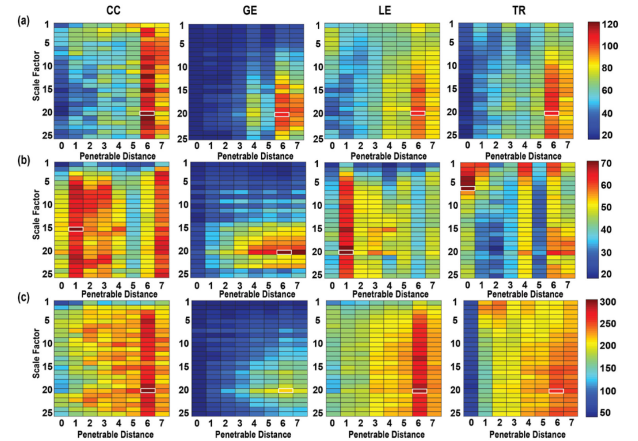


Fig. 5. F-values of CC, GE, LE and TR for (a) CP-I (b) CP-II and (c) CP-III.

be noted that we varied both ρ and SF within the above specified range because for higher values of ρ and SF , we noticed a decline in performance which may be caused due to loss of significant signal information. Hence, those results are not reported here.

A. Binary Class Comparison

To understand the effect of the parameters in details, we analyzed the WVG performance for pair wise groups of the three binary classes in Fig. 5. We observe that for each CP, the F-values of the selected features are different from each other and depend on both ρ and SF when varied within a specified range. The general trend is that with the increase in both ρ and SF , F-values of all the features are found to increase with the exception being CP-II, where we observe that higher F-values are obtained at lower values of ρ for CC, LE and TR features respectively. However, for the GE all three CPs, GE feature.

Shows a similar trend, while rest of the features show relatively widespread variation in F-values for all the CPs. Also, the effect of ρ and SF are not independent of each other. We performed multi-way ANOVA test to study the interaction effect between ρ and SF and we obtained a significant interaction effect ($p = 0.0003$) between them. Based on the above variation, we determined the optimum parameter values for WVG construction and subsequent feature selection. For CP-I and CP-III, we selected optimal parameters (marked in white in Fig. 5) $\rho = 6$ and $SF = 20$. For CP-II, we selected $SF = 15$ and $\rho = 1$ for evaluating CC, $SF = 20$ and $\rho = 6$ for GE, $SF = 20$ and $\rho = 1$ for LE and $SF = 6$ and $\rho = 0$ for TR, respectively.

B. Multi-Class Comparison

Fig. 6 shows the F-values obtained for CP-IV. For GE and TR, lower values of ρ and SF yielded lower F-values. But the F-value increases with the increase in ρ and SF for all features. Detailed observation revealed that for GE the variation is exactly similar to the binary class. However, unlike GE and feature the trend is similar to the other CPs. Interestingly, for TR for CC and LE, the result is widespread. For CP-IV, the highest F-value (marked in white in Fig. 6) for all the features is obtained for

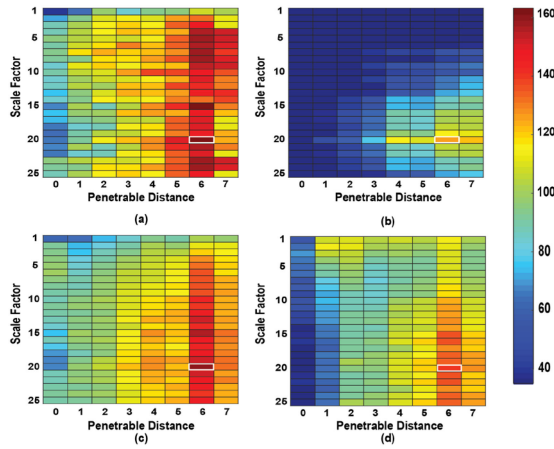


Fig. 6. F-values of (a) CC (b) GE (c) LE and (d) TR for CP-IV.

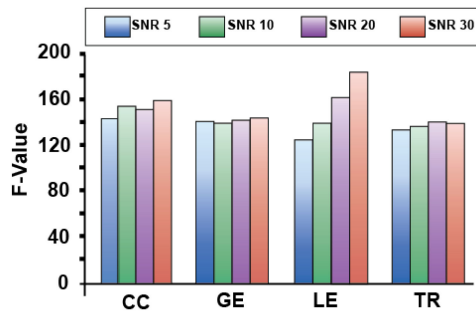


Fig. 7. Variation of highest F-value for the four features with noise for $\rho = 6$ and $SF = 20$.

$SF = 20$ and $\rho = 6$. Therefore, it can be concluded that, although the effect of parameter variation is different for different features, yet the parameters finally converge to a particular value where the difference between the classes is maximum for all the features.

C. Influence of Noise

In the earlier sections (subsections A and B), we determined the optimum values of ρ and SF depending on the highest F-values of the four features obtained from ANOVA test. In order to show whether the influence of noise can alter optimum parameter selection, we added white Gaussian noise of different signal to noise ratios (SNR) to the MUAP signal. Then we constructed WVG with pre-determined optimum values of $SF = 20$ and $\rho = 6$ and observed if there is any change in the F-value for different features due to addition of noise. The results are shown in Fig. 7.

It can be observed that for CC, TR and GE, addition of noise does not perturb the overall discriminability (highest F-value is almost constant) to a great extent. But LE is comparatively more sensitive to noise than the other features. This is because of the inherent property of the LE feature which is dependent on local clusters. Adding noise increases the number of local clusters causing the performance of LE to decline. Based on above observation, it can be said that for majority of the features, maximum F-value is unperturbed with the increase in SNR indicating that the selected parameters of WVG are robust

TABLE II
CLASSIFICATION ACCURACY FOR DIFFERENT CPs

CP	Accuracy	Specificity	Sensitivity	Precision
I	98.57 \pm 1.23	97.86 \pm 1.84	100.00 \pm 0	96.00 \pm 3.44
II	98.09 \pm 1.88	97.14 \pm 2.82	100.00 \pm 0	94.83 \pm 4.98
III	99.45 \pm 0.66	98.78 \pm 2.50	100.00 \pm 0	97.42 \pm 4.45
IV	99.05 \pm 0.29	98.57 \pm 1.43	100.00 \pm 0	97.33 \pm 3.44

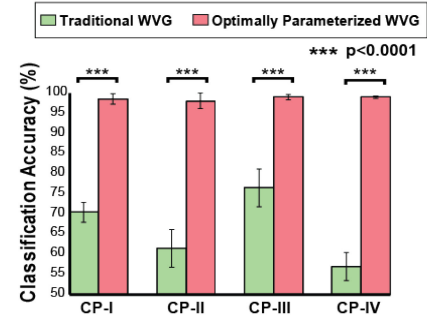


Fig. 8. Comparison between traditional and optimally parameterized WVG using NB classifier.

against noise. However, there is no clear relationship between SNR and selection of WVG parameters solely depends on the type of signal to be analyzed. The optimally selected WVG parameters were found to be robust when SNR is varied within a permissible range. However, if the noise level is very high, a higher value of ρ and SF and will give better performance. This is because higher ρ will enable WVG to penetrate one or more data points with large amplitudes. Similarly, higher SF will have better smoothing effect making the system less sensitive against noise.

D. Classification Results Using NB Classifier

The optimal combination of ρ and SF that yielded highest F-values for all the features were selected and classification of EMG signals was done using the corresponding feature values. All classification accuracy was obtained by using 10 fold cross validation for 10 iterations and the mean classification accuracy with standard deviation is reported. Table II shows the classification results for the four CPs obtained using NB classifier. We observed that the mean classification accuracy of 98.57%, 98.09%, 99.45% and 99.05% for CP-I, CP-II, CP-III and CP-IV, respectively. Besides, we also obtained 100% sensitivity for all four CPs. Therefore, we can say that optimally parameterized WVG can accurately detect EMG signals. The performance of the proposed method is also compared with traditional WVG algorithm and the results are shown in Fig. 8.

We observe that for all CPs a significant improvement in the classification performance (***) shows significant difference based on Student's *t*-test with probability value (p) < 0.0001 is obtained. Prior to *t*-test, we performed the Anderson Darling test on all the features between three groups (for all ρ and SF values) and found that all of them are normally distributed ($p > 0.1$). From the experimental observations, we can infer that optimally parameterized WVG has delivered better performance in discriminating EMG signals compared to traditional WVG.

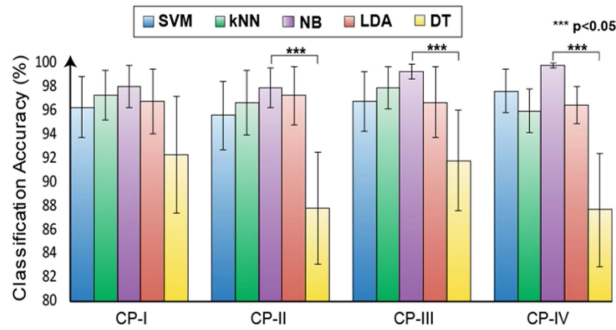


Fig. 9. Classification comparison of other classifiers.

TABLE III
REDUCTION OF COMPUTATIONAL TIME (SECONDS)

Feature	WVG	DWT	(EMD)	Optimally parameterized WVG
CC	4.53	2.78	3.45	0.70
GE	3.54	2.15	2.65	0.63
LE	2.22	1.74	2.14	0.15
TR	2.46	1.65	1.98	0.10

E. Classification Results Using Other Classifiers

We compared the performance of the proposed method using five widely used machine learning classifiers namely support vector machines (SVM), k-nearest neighbors (kNN), naïve bayes (NB), linear discriminant analysis (LDA) and decision trees (DT). The classification performance of different classifiers is shown in Fig. 9. The optimum classifier parameters were selected using grid search algorithm. In the case of SVM, linear kernel was used for CP-I and CP-IV, whereas RBF kernel delivered best performance for CP-II and CP-III, respectively. In the case of kNN classifier, Euclidean distance was used and the corresponding values of k for four CPs were selected as 5, 3, 7, and 9, respectively. One-way ANOVA showed significant difference for all CPs ($p < 0.0001$). NB outperformed all the classifiers in all the CPs. Tukey-Kramer post-hoc analysis revealed that the DT classifiers performs significantly worse than all the other classifiers. However, we did not observe significant difference between the other four classifiers indicating that the performance of optimally parameterized WVG is robust.

F. Reduction in Computational Time

Along with high classification accuracy, we were also able to significantly reduce the computational time. Computational time is an important parameter for any computer aided disease diagnosis system. From existing literature [18] we know that when the analyzed signal contains large number of data points, then computation of conventional WVG takes significantly long time which is undesirable from the practical point of view. Since our proposed method can be potentially implemented for real-time detection of neuromuscular disorders, hence computational time is a crucial parameter. Table III shows the computational time required to extract each feature using the proposed method

in comparison with conventional WVG as well as with some existing state of the art methods.

We can observe from Table III that using optimally selected WVG parameters, significant reduction in computational time has been observed for all the features. In comparison with conventional WVG, 96% reduction in computational time was observed for extracting the TR feature, followed by LE and CC which showed 93.3% and 83.75% reduction respectively. The reduction in computation time for extracting the GE feature is 75%. In comparison with DWT (Daubechies-4) and EMD also, we observed that our proposed method is computationally inexpensive. Between EMD and DWT, the time required to extract all the features in higher in the case of EMD. This is because, EMD iteratively extracts IMF's from a given signal which makes it inadvertently computationally expensive than DWT as well as the proposed method. Using optimally parameterized WVG, the reduction in computational time is caused due to the reduction in number of nodes of the graph due to change in SF values. It is to be mentioned here that computational time for all the cases is calculated in MATLAB R2014a (8.3) environment on an Intel core i5 machine with 2.40 GHz processor and 8 GB RAM.

V. DISCUSSIONS

In this present work we have explored the effect of varying ρ and SF , in an optimized combination for classification of neuromuscular diseases. Our primary goal in the paper was not only to propose neuromuscular disease detection framework, but also to explore the role of the WVG parameters on its performance. The connectivity between different nodes (data points) of the graph is represented by an adjacency matrix which is depicted in Fig. 10.

A. Role of the Parameters in WVG Performance

We observed that the performance of WVG significantly improved by altering the values of ρ and SF in few specific combinations. Also, the trend of the performance variation was not similar for different classification problems. Hence, we tried to untangle the complex relationship between the WVG parameters and the MUAP signal patterns, which is rooted to the physiology of the neuromuscular diseases. Based on previous literatures, it is known that there are significant dissimilarities in motor unit firing patterns among ALS, myopathy and healthy individuals. For a healthy subject, a relatively regular firing pattern of motor unit discharge can be observed, whereas for ALS, the loss of motor neurons results in irregular firing pattern (increased amplitude and duration) [30]. For myopathy, caused by the dysfunction of skeletal muscles, the MUAPs are characterized by decreased amplitude and successive firing patterns. Therefore, characterizing the MUAP pattern within that short time interval can successfully aid in detection of the neuromuscular diseases. The WVG is capable of capturing such state of a signal within short time duration [31]. The explanation for such capability lies in the theoretical definition of the WVG. One node (or data point) is connected to another node by an edge, only when one node has a relatively higher magnitude than other node, with no other nodes in between them with

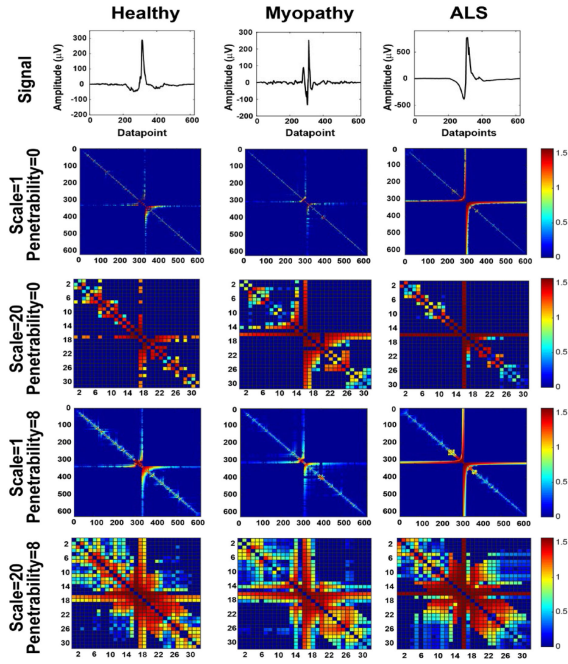


Fig. 10. MUAP for the healthy, myopathy and ALS signals (top row). Variation of WVG adjacency matrix for different combinations of ρ and SF .

comparable magnitude. This gets highly disrupted in presence of noise or even for higher baseline activity. For instance, in case of a healthy MUAP, which is comprised of a single sharp spike, the high magnitude nodes during the firing of the muscle fibers ('firing nodes') should be connected to all the nodes before the firing occurred ('non-firing nodes'). In presence of small noises, even before the actual firing takes place, it can block a possible edge to the spike nodes (Fig. 10). Therefore, with increase in the value of ρ , the non-firing nodes will be more connected to the firing nodes, thereby resulting in higher local clusters. This phenomenon can be clearly observed in Fig. 10, where for $\rho = 8$, the firing nodes (310-350) are strongly connected to the non-firing nodes. For ALS, these local clusters are more observed only near the firing neurons with much higher magnitude owing to the characteristics of the ALS MUAPs [32]. Therefore, the CC, LE and TR features could easily discriminate the ALS MUAP from the healthy and myopathy MUAPs, when the value of ρ was increased with not much effect of the SF value.

Discriminating between healthy and myopathy MUAPs is relatively more challenging as the magnitude of the MUAP is comparable. Although successive firings characterize a myopathy MUAP, a relative larger spike with comparable magnitude gives similar local clusters (Fig. 10, adjacency matrix for $SF = 1$ and $\rho = 0$). Increasing the value of ρ helped to eliminate the effect of the noise in the non-firing nodes. On the other hand, increasing the SF increased the clustering among the firing nodes at the global level, which is relatively larger, compared to healthy and ALS due to the multiple firing pattern in myopathy. Therefore, we observed better performance with higher value of ρ and SF for the GE feature.

TABLE IV
COMPARATIVE STUDY WITH EXISTING LITERATURES

CP	Method	Accuracy (%)
I	Mel Frequency cepstral coefficient+kNN [5]	92.8
	DWT+ Canonical Correlation Analysis + kNN [33]	97.6
	TQWT+ Random forest [9]	89.16
	Two-fold feature extraction + Canonical Correlation Analysis [34]	95.58
	Optimally parameterized WVG	98.57
II	DWT + Canonical Correlation Analysis + kNN [33]	96.6
	TQWT+ Random forest [9]	82.41
	Two-fold feature extraction + Canonical Correlation Analysis [34]	95.91
	Optimally parameterized WVG	98.09
III	TQWT + Random forest [9]	94.42
	Optimally parameterized WVG	99.45
IV	DWT, Fuzzy Entropy + Artificial Neural Network [35]	98
	Dominant MUAP, DWT + kNN [2]	98.8
	DWT + Canonical Correlation Analysis + kNN [33]	98.8
	Normalized weighted vertical visibility algorithm + SVM [19]	98.36
	Ensemble EMD + LDA [36]	98
	Optimally parameterized WVG	99.05

B. Comparative Study With Existing Literatures

In Table IV, the performance of our proposed method is compared with some existing methods already proposed for detection of neuromuscular diseases. From Table IV we can observe that for all the four CPs our proposed method delivered better performance than the existing methods. Moreover, it should be noted that by using traditional WVG, the recent study in [19] has achieved 98.36% accuracy for CP-IV using a large number of network features. Using the proposed method, we achieved better classification accuracy for CP-IV compared to [19] and also, the size of the feature pool used in this study is smaller in comparison with [19]. Besides, from Table III, we observed the computational cost of our proposed method is lower than the traditional signal processing methods. So, we can infer that optimal selection of WVG parameters results in comparable and even better accuracy in EMG signal classification with reduced computational time.

VI. CONCLUSION

In this paper, we have shown the effect of ρ and SF on the WVG of EMG signals for discrimination of neuromuscular disorders. Our analysis showed that both the parameters significantly change the WVG performance for both binary and multi-class classification problem. Based on the features derived from the optimized combination of two WVG parameters, we have observed a significant increase in classification performance compared to the traditional WVG. Along with improved classification accuracy, the computational time was also significantly reduced thereby making it practically suitable for real-time operation. We also observed that the parameters are least affected by presence of noise but are sensitive to the change in MUAP patterns. NB classifier showed the highest

classification accuracy, however, SVM, LDA and kNN also showed comparative performances. Our proposed optimally parameterized WVG can therefore be applied for clinical diagnosis of neuromuscular disorders. In future, our observation can be extended further to analyze other physiological signals like electroencephalography (EEG), magnetoencephalography (MEG) etc.

REFERENCES

- [1] R. Bose, K. Samanta, and S. Chatterjee, "Cross-correlation based feature extraction from EMG signals for classification of neuro-muscular diseases," in *Proc. IEEE Int. Conf. Intell. Control Power Instrum.*, Kolkata, India, 2016, pp. 241–245.
- [2] A. B. M. S. U. Doulah, S. A. Fattah, W. P. Zhu, and M. O. Ahmad, "Wavelet domain feature extraction scheme based on dominant motor unit action potential of EMG signal for neuromuscular disease classification," *IEEE Trans. Biomed. Circuits Syst.*, vol. 8, no. 2, pp. 155–164, Apr. 2014.
- [3] C. S. Pattichis and A. G. Elia, "Autoregressive and cepstral analyses of motor unit action potentials," *Med. Eng. Phys.*, vol. 21, no. 6–7, pp. 405–419, 1999.
- [4] N. F. Güler and S. Koçer, "Classification of EMG signals using PCA and FFT," *J. Med. Syst.*, vol. 29, no. 3, pp. 241–250, 2005.
- [5] A. Doulah and S. Fattah, "Neuromuscular disease classification based on mel frequency cepstrum of motor unit action potential," in *Proc. Int. Conf. Elect. Eng. Inf. Commun. Technol.*, 2014, pp. 1–4.
- [6] A. Sengur, M. Gedikpinar, Y. Akbulut, E. Deniz, V. Bajaj and Y. Guo, "DeepEMGNet: An application for efficient discrimination of ALS and normal EMG signals," in *Proc. Springer Int. Conf. Mechatronics*, Springer, Cham, 2017, pp. 619–625.
- [7] A. Sengur, Y. Akbulut, Y. Guo, and V. Bajaj, "Classification of amyotrophic lateral sclerosis disease based on convolutional neural network and reinforcement sample learning algorithm," *Health Inf. Sci. Syst.*, vol. 5, no. 1, pp. 1–7, 2017.
- [8] S. Chatterjee, K. Samanta, N. Ray Choudhury, and R. Bose, "Detection of myopathy and ALS electromyograms employing modified window stockwell transform," *IEEE Sensors Lett.*, vol. 3, no. 7, Jul. 2019, Art. no. 7001204.
- [9] D. Joshi, A. Tripathi, R. Sharma, and R. B. Pachori, "Computer aided detection of abnormal EMG signals based on tunable-Q wavelet transform," in *Proc. IEEE 4th Int. Conf. Signal Process. Integr. Netw.*, Noida, India, 2017, pp. 544–549.
- [10] V. K. Mishra, V. Bajaj, A. Kumar, and G. K. Singh, "Analysis of ALS and normal EMG signals based on empirical mode decomposition," *IET Sci., Meas. Technol.*, vol. 10, no. 8, pp. 963–971, 2016.
- [11] X. Zhang, X. Chen, P. E. Barkhaus, and P. Zhou, "Multiscale entropy analysis of different spontaneous motor unit discharge patterns," *IEEE J. Biomed. Health Informat.*, vol. 17, no. 2, pp. 470–476, Mar. 2013.
- [12] U. R. Acharya, E. Y. K. Ng, G. Swapnaand, and Y. S. L. Michelle, "Classification of normal, neuropathic and myopathic electromyograph signals using nonlinear dynamics method," *J. Med. Imag. Health Informat.*, vol. 1, no. 4, pp. 375–380, 2011.
- [13] W. Ren, and N. Jin, "Vector visibility graph from multivariate time series: a new method for characterizing nonlinear dynamic behavior in two-phase flow," *Nonlinear Dyn.*, vol. 97, pp. 2547–2556, 2019.
- [14] W. Ren and N. Jin, "Sequential limited penetrable visibility-graph motifs," *Nonlinear Dyn.*, vol. 99, pp. 2399–2408, 2020.
- [15] L. Lacasa, B. Luque, F. Ballesteros, J. Luque, and J. C. Nuno, "From time series to complex networks: The visibility graph," *Proc. Nat. Acad. Sci.*, vol. 105, no. 13, pp. 4972–4975, 2008.
- [16] S. Supriya, S. Siuly, H. Wang, J. Cao, and Y. Zhang, "Weighted visibility graph with complex network features in the detection of epilepsy," *IEEE Access*, vol. 4, pp. 6554–6566, 2016.
- [17] G. Zhu, Y. Li, and P. P. Wen, "Epileptic seizure detection in EEGs signals using a fast weighted horizontal visibility algorithm," *Comput. Methods Programs Biomed.*, vol. 115, no. 2, pp. 64–75, 2014.
- [18] S. Supriya, S. Siuly, H. Wang, and Y. Zhang, "EEG sleep stages analysis and classification based on weighed complex network features," *IEEE Trans. Emerg. Topics Comput. Intell.*, pp. 1–11, 2018.
- [19] P. Artameeyanant, S. Sultornsanee, and K. Chamnongthai, "An EMG-based feature extraction method using a normalized weight vertical visibility algorithm for myopathy and neuropathy detection," *SpringerPlus*, vol. 5, no. 1, 2016, Art. no. 2101.
- [20] Z. T. T. J. Ning-De, and G. Z. K. L. Y. Bin, "Limited penetrable visibility graph for establishing complex network from time series," *Acta Physica Sinica*, vol. 61, no. 3, 2012, Art. no. 030506.
- [21] Z. K. Gao, L. D. Hu, T. T. Zhou, and N. D. Jin, "Limited penetrable visibility graph from two-phase flow for investigating flow pattern dynamics," *Acta Physica Sinica -Chinese Ed.*, vol. 62, no. 11, 2013, Art. no. 110507.
- [22] Z. K. Gao, Q. Cai, Y. X. Yang, W. D. Dang, and S. S. Zhang, "Multiscale limited penetrable horizontal visibility graph for analyzing nonlinear time series," *Scientific Rep.*, vol. 6, 2016, Art. no. 35622.
- [23] M. Costa, A. L. Goldberger, and C. K. Peng, "Multiscale entropy analysis of complex physiologic time series," *Physical Rev. Lett.*, vol. 89, no. 6, 2002, Art. no. 068102.
- [24] M. Nikolic, "Detailed analysis of clinical electromyography signals: EMG decomposition, findings and firing pattern analysis in controls and patients with myopathy and amyotrophic lateral sclerosis," Ph.D. dissertation, Univ. Copenhagen, Denmark, Aug. 2001.
- [25] K. C. McGill, Z. C. Lateva and H. R. Marateb, "EMGLAB: An interactive EMG decomposition program," *J. Neurosci. Methods*, vol. 149, no. 2, pp. 121–133, 2005.
- [26] J. Saramäki, M. Kivelä, J.-P. Onnela, K. Kaski, and J. Kertesz, "Generalizations of the clustering coefficient to weighted complex networks," *Physical Rev. E*, vol. 75, no. 2, 2007, Art. no. 027105.
- [27] V. Latora and M. Marchiori, "Efficient behavior of small-world networks," *Physical Rev. Lett.*, vol. 87, no. 19, 2001, Art. no. 198701.
- [28] X. Liu, R. Lu, J. Ma, L. Chen, and B. Qin, "Privacy-preserving patient-centric clinical decision support system on naive Bayesian classification," *IEEE J. Biomed. Health Informat.*, vol. 20, no. 2, pp. 655–668, 2015.
- [29] R. Bose, K. Samanta, S. Chatterjee, S. Bhattacharyya, and A. Khasnobish, "Motor imagery classification enhancement with concurrent implementation of spatial filtration and modified stockwell transform," in *Bioelectronics and Medical Devices*, ed. Amsterdam, The Netherlands: Elsevier, 2019, pp. 793–817.
- [30] M. de Carvalho, A. Eisen, C. Krieger, and M. Swash, "Motoneuron firing in amyotrophic lateral sclerosis (ALS)," *Frontiers Human Neurosci.*, vol. 8, 2014, Art. no. 719.
- [31] R. J. Barohn, M. M. Dimachkie, and C. E. Jackson, "A pattern recognition approach to patients with a suspected myopathy," *Neurologic Clinics*, vol. 32, no. 3, pp. 569–593, 2014.
- [32] M. Stephen, C. Gu, and H. Yang, "Visibility graph based time series analysis," *PloS One*, vol. 10, no. 11, pp. 1–19, 2015.
- [33] A. Hazarika, L. Dutta, M. Boro, M. Barthakur, and M. Bhuyan, "An automatic feature extraction and fusion model: Application to electromyogram (EMG) signal classification," *Int. J. Multimedia Inf. Retrieval*, vol. 7, no. 3, pp. 173–186, 2018.
- [34] A. Hazarika, L. Dutta, M. Barthakur, and M. Bhuyan, "Two-fold feature extraction technique for biomedical signals classification," in *Proc. Int. Confe. Inventive Comput. Technol.*, 2016, vol. 2, pp. 1–4.
- [35] M. Vallejo, C. J. Gallego, L. Duque-Muñoz, and E. Delgado-Trejos, "Neuromuscular disease detection by neural networks and fuzzy entropy on time-frequency analysis of electromyography signals," *Expert Syst.*, vol. 35, no. 4, 2018, Art. no. e12274.
- [36] G. R. Naik, S. E. Selvan, and H. T. Nguyen, "Single-channel EMG classification with ensemble-empirical-mode-decomposition-based ICA for diagnosing neuromuscular disorders," *IEEE Trans. Neural Syst. Rehabil. Eng.*, vol. 24, no. 7, pp. 734–743, Jul. 2016.